Nonlinear Model Order Reduction of a Variable Reluctance Stepper Motor Using the Parameterized Cauer Ladder Network Method

Miwa Tobita[1], and Tetsuji Matsuo[1]
[1] Graduate School of Engineering, Kyoto University, Kyoto 6158510, Japan

The parameterized Cauer ladder network (CLN) method, which is a recently developed nonlinear model order reduction method, was applied to the analysis of a variable reluctance stepper motor. To represent the magnetic saturation, we parameterized the stator network using the coil magnetic flux and input sequence. The rotor network adopted the CLN to investigate the effect of the eddy current. The CLN method was effective in analyzing the continuous rotation, stepwise rotation, and step-out motion.

***Index Terms*—Nonlinear model order reduction, variable reluctance stepper motor, parameterized Cauer ladder network, eddy currents, magnetic saturation.**

I. Introduction

Owing to the limited availability of rare-earth elements, variable reluctance (VR) motors, such as VR stepper motors, are expected to be in high demand in the coming decades. The control of these motors requires fast transient analyses with high accuracy. Model order reduction (MOR) methods have been widely studied to obtain reduced systems that satisfy this requirement [1]–[3].

The Cauer ladder network (CLN) method, a recently developed MOR method, can be a powerful tool for simulating motor dynamics. It reduces the electromagnetic field of machines to the circuit elements of the CLN. The reduction is based on spatial mode decomposition, wherein the orthogonal bases are systematically produced from the CLN recurrence formula [4]. The CLN method was extended to a multi-port model and applied to the analysis of induction motors [5]. Later, the nonlinear magnetic characteristics were incorporated using the parameterized CLN method [6].

This study applies the parameterized multi-port CLN method to a VR stepper motor. The reduced model represents the magnetic saturation of the stator and the effect of the eddy current in the rotor. Without any additional offline preparations, the CLN method can analyze the transient stepwise motion and step-out behavior, which should be investigated to evaluate the control methods of VR stepper motors.

II. Parameterized CLN Method

Fig. 1 provides an overview of the motor analysis using the parameterized CLN method. First, the stator and rotor networks are prepared in the offline calculation (Section II-B and II-C), and then the online calculation is performed (Section II-D and II-E).

A. Basic equations of the CLN Method

We assume that the variable vectors of the magnetic vector potential $\boldsymbol{a}$ and electric field $\boldsymbol{e}$ in the finite element (FE) space satisfy the governing equations of the eddy-current field,

$$\boldsymbol{K}\boldsymbol{a} = \boldsymbol{\sigma}\boldsymbol{e}, \quad \boldsymbol{C}\boldsymbol{e} = -\frac{\mathrm{d}}{\mathrm{d}t}\boldsymbol{C}\boldsymbol{a}, \tag{1}$$

Corresponding author: M. Tobita (email: tobita.miwa.73x@kyoto-u.jp).

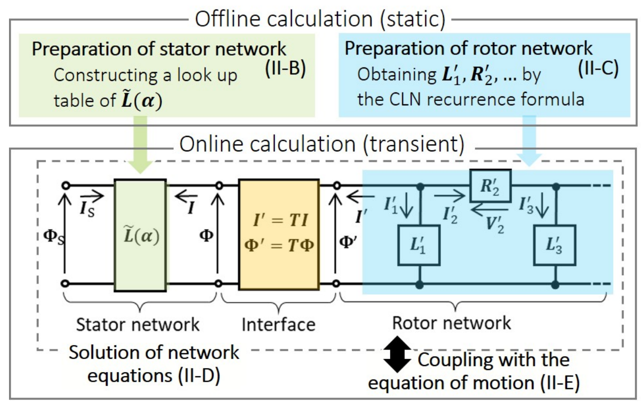

Fig. 1. Overview of the motor analysis using the parameterized CLN method.

where $\boldsymbol{K} = \boldsymbol{C}^{\mathrm{T}}\boldsymbol{\nu}\boldsymbol{C}$ is the stiffness matrix, and $\boldsymbol{C}$ is the edge-face incidence matrix; $\boldsymbol{\sigma}$ and $\boldsymbol{\nu}$ are the conductivity and reluctivity matrices, respectively, defined in the FE space.

Let $\boldsymbol{I}_{2n-1}, \boldsymbol{V}_{2n} \in \mathbb{R}^M$ $(n = 1, 2, \cdots)$ be the state vectors of the current and voltage, respectively, at the nth stage of the M-port ladder network. We assume $\boldsymbol{a}$ and $\boldsymbol{e}$ are decomposed as

$$\boldsymbol{a} = \sum_n \boldsymbol{a}_{2n-1}\boldsymbol{I}_{2n-1}, \quad \boldsymbol{e} = \sum_n \boldsymbol{e}_{2n}\boldsymbol{V}_{2n}, \tag{2}$$

where $\boldsymbol{a}_{2n-1} = [\boldsymbol{a}_{1,2n-1}, \boldsymbol{a}_{2,2n-1}, \cdots, \boldsymbol{a}_{M,2n-1}]$ and $\boldsymbol{e}_{2n} = [\boldsymbol{e}_{1,2n}, \boldsymbol{e}_{2,2n}, \cdots, \boldsymbol{e}_{M,2n}]$, and $\boldsymbol{a}_{m,2n-1}$ and $\boldsymbol{e}_{m,2n}$ are the basis vectors of the magnetic vector potential and electric field, respectively, when a unit input is provided only to the mth port [5]. The state equations of the ladder network are

$$\boldsymbol{V}_{2n} = \boldsymbol{L}_{2n-1}\frac{\mathrm{d}\boldsymbol{I}_{2n-1}}{\mathrm{d}t} - \boldsymbol{L}_{2n+1}\frac{\mathrm{d}\boldsymbol{I}_{2n+1}}{\mathrm{d}t}, \tag{3}$$

$$\boldsymbol{I}_{2n+1} = \boldsymbol{R}_{2n}^{-1}\boldsymbol{V}_{2n} - \boldsymbol{R}_{2n+2}^{-1}\boldsymbol{V}_{2n+2}, \tag{4}$$

where $\boldsymbol{L}_{2n-1}$ and $\boldsymbol{R}_{2n}$ are the inductance and resistance matrices of the CLN, respectively.

With the assumption of the mode decomposition (2), the recurrence formula [4] is derived from (1), (3), and (4) as

$$\boldsymbol{K}(\boldsymbol{a}_{2n+1}-\boldsymbol{a}_{2n-1})=\boldsymbol{\sigma}\boldsymbol{e}_{2n}\boldsymbol{R}_{2n}, \tag{5}$$

$$\boldsymbol{e}_{2n+2}-\boldsymbol{e}_{2n}=-\boldsymbol{a}_{2n+1}\boldsymbol{L}_{2n+1}^{-1}, \tag{6}$$

where $\boldsymbol{L}_{2n-1}=\boldsymbol{a}_{2n-1}^{\mathrm{T}}\boldsymbol{K}\boldsymbol{a}_{2n-1}$ and $\boldsymbol{R}_{2n}^{-1}=\boldsymbol{e}_{2n}^{\mathrm{T}}\boldsymbol{\sigma}\boldsymbol{e}_{2n}$. We use the initial conditions $\boldsymbol{e}_0=\boldsymbol{0}$ and $\boldsymbol{K}\boldsymbol{a}_1=\boldsymbol{j}_{\mathrm{unit}}$ assuming a unit source $\boldsymbol{j}_{\mathrm{unit}}=[\boldsymbol{j}_1,\boldsymbol{j}_2,\cdots,\boldsymbol{j}_m,\cdots,\boldsymbol{j}_{\mathrm{M}}]$ is provided, where $\boldsymbol{j}_m$ is an input vector discretized in the FE space when a unit power input is given only to the mth port. By solving (5) and (6) with the initial conditions, we can systematically obtain $\boldsymbol{L}_{2n-1}$ and $\boldsymbol{R}_{2n}$.

B. Preparation of the stator network

Generally, VR stepper motors are driven by a voltage source. However, we assume a current source drive to simulate the motor behavior separately from the power supply. A voltage source drive can also be analyzed using the method described below by adding the stator winding resistance to the stator network.

For simplicity, we assume that the stator iron core is laminated, and its conductivity is zero. Hence, the stator network comprises a single-stage nonlinear inductance $\tilde{\boldsymbol{L}}(\boldsymbol{\alpha})$, where $\boldsymbol{\alpha}$ is the parameter vector representing the nonlinear magnetic characteristics. The network equation [5] [6] is

$$\tilde{\boldsymbol{\Phi}}=\begin{bmatrix}\boldsymbol{L}_{00}(\boldsymbol{\alpha}) & \boldsymbol{L}_{10}^{\mathrm{T}}(\boldsymbol{\alpha})\\ \boldsymbol{L}_{10}(\boldsymbol{\alpha}) & \boldsymbol{L}_{11}(\boldsymbol{\alpha})\end{bmatrix}\tilde{\boldsymbol{I}}=\tilde{\boldsymbol{L}}(\boldsymbol{\alpha})\tilde{\boldsymbol{I}}, \tag{7}$$

where $\tilde{\boldsymbol{I}}=[\boldsymbol{I}_{\mathrm{s}},\boldsymbol{I}]^{\mathrm{T}}$ and $\tilde{\boldsymbol{\Phi}}=[\boldsymbol{\Phi}_{\mathrm{s}},\boldsymbol{\Phi}]^{\mathrm{T}}$. Here, $\boldsymbol{I}_{\mathrm{s}}=[I_{\mathrm{U}},I_{\mathrm{V}},I_{\mathrm{W}}]^{\mathrm{T}}$ and $\boldsymbol{\Phi}_{\mathrm{s}}=[\Phi_{\mathrm{U}},\Phi_{\mathrm{V}},\Phi_{\mathrm{W}}]^{\mathrm{T}}$ are the three-phase current and magnetic flux vectors, respectively. The vectors $\boldsymbol{I}$ and $\boldsymbol{\Phi}$ are defined as

$$\boldsymbol{I}=[H_{\mathrm{c}1},H_{\mathrm{s}1},H_{\mathrm{c}3},H_{\mathrm{s}3},\cdots,H_{\mathrm{c}2K-1},H_{\mathrm{s}2K-1}]^{\mathrm{T}}, \tag{8}$$

$$\boldsymbol{\Phi}=\frac{\pi r_{\mathrm{c}}}{p}[A_{\mathrm{c}1},A_{\mathrm{s}1},A_{\mathrm{c}3},A_{\mathrm{s}3},\cdots,A_{\mathrm{c}2K-1},A_{\mathrm{s}2K-1}]^{\mathrm{T}}, \tag{9}$$

where $H_{\mathrm{c}2k-1}$ (or $H_{\mathrm{s}2k-1}$) and $A_{\mathrm{c}2k-1}$ (or $A_{\mathrm{s}2k-1}$) are the $2k-1$th cosine (or sine) Fourier spatial harmonic components of the stator-side axial vector potential A_z and circumferential magnetic field H_ϕ, respectively, on the interface; $2K$ is the number of harmonics considered; p is the number of pole pairs; and r_{c} is the radius of the interface.

The CLN method was applied in [6] to the induction motor analysis assuming the three-phase balanced current source. This study analyzes a one-phase-on operation by switching three current inputs

$$\boldsymbol{I}_{\mathrm{s}}(\boldsymbol{\alpha})=\begin{cases}[I_{\mathrm{src}},0,0]^{\mathrm{T}} & (q=1),\\ [0,I_{\mathrm{src}},0]^{\mathrm{T}} & (q=2),\\ [0,0,I_{\mathrm{src}}]^{\mathrm{T}} & (q=3),\end{cases} \tag{10}$$

where $\boldsymbol{\alpha}=(I_{\mathrm{src}},q)$, I_{src} is the amplitude of the current source, and q is the input index. Although it is outside the scope in this study, a micro-step operation with any phase number can be handled by assigning the index q to the possible inputs.

For the computation of $\tilde{\boldsymbol{L}}(\boldsymbol{\alpha})$, first, the nonlinear reluctivity matrix $\boldsymbol{\nu}$ is determined by solving the magnetostatic equation $\boldsymbol{C}^{\mathrm{T}}\boldsymbol{\nu}\boldsymbol{C}\boldsymbol{a}=\boldsymbol{j}_{\mathrm{s}}(\boldsymbol{\alpha})$ [6]. Here, $\boldsymbol{\nu}$ is a function of the magnetic flux density $\boldsymbol{C}\boldsymbol{a}$, and $\boldsymbol{j}_{\mathrm{s}}(\boldsymbol{\alpha})$ is a variable vector of the current source density when $\boldsymbol{I}_{\mathrm{s}}(\boldsymbol{\alpha})$ is given to the coils. Then, $\boldsymbol{a}_1$ is derived with the determined $\boldsymbol{\nu}$ by solving $\boldsymbol{C}^{\mathrm{T}}\boldsymbol{\nu}\boldsymbol{C}\boldsymbol{a}_1=\boldsymbol{j}_{\mathrm{unit}}$, and $\tilde{\boldsymbol{L}}(\boldsymbol{\alpha})=\boldsymbol{a}_1^{\mathrm{T}}\boldsymbol{C}^{\mathrm{T}}\boldsymbol{\nu}\boldsymbol{C}\boldsymbol{a}_1$ is obtained.

Reference [6] revealed that the preferred parameter to achieve high accuracy is either the magnetic flux interlinking the coils or the flux on the gap interface, but not the current source. Therefore, we transform the parameter of $\tilde{\boldsymbol{L}}$ from $\boldsymbol{\alpha}=(I_{\mathrm{src}},q)$ to (Φ_{coil},q), where Φ_{coil} is the amplitude of the coil flux obtained by

$$\Phi_{\mathrm{coil}}=\sqrt{\frac{2}{3}}||\boldsymbol{\Phi}_{\mathrm{s}}||_2=\sqrt{\frac{2}{3}(\Phi_{\mathrm{U}}^2+\Phi_{\mathrm{V}}^2+\Phi_{\mathrm{W}}^2)}. \tag{11}$$

In the offline preparation of $\boldsymbol{L}_{00}(\boldsymbol{\alpha})$, the relation between $\boldsymbol{\Phi}_{\mathrm{s}}$ and $\boldsymbol{I}_{\mathrm{s}}$ is computed by $\boldsymbol{\Phi}_{\mathrm{s}}=\boldsymbol{L}_{00}(\boldsymbol{\alpha})\boldsymbol{I}_{\mathrm{s}}$, which is derived from (7) under the condition that $\boldsymbol{I}=\boldsymbol{0}$.

C. Preparation of the rotor network

The rotor CLN consists of the inductance and resistance matrices $\boldsymbol{L}_1',\boldsymbol{R}_2',\boldsymbol{L}_3',\cdots$, which are obtained by solving (5) and (6) in the rotor domain of the FE space. The computation is completed separately from II-B.

The network equations of the rotor [5] are

$$\boldsymbol{L}_{2n-1}'\frac{\mathrm{d}\boldsymbol{I}_{2n-1}'}{\mathrm{d}t}-\boldsymbol{L}_{2n+1}'\frac{\mathrm{d}\boldsymbol{I}_{2n+1}'}{\mathrm{d}t}=\boldsymbol{R}_{2n}'\boldsymbol{I}_{2n}', \tag{12}$$

and $\boldsymbol{I}_{2n}'=-\boldsymbol{I}'-\boldsymbol{I}_1'\cdots-\boldsymbol{I}_{2n-1}'$, where $\boldsymbol{I}_{2n-1}'$ is the state vector of the current flowing through $\boldsymbol{L}_{2n-1}'$ (see the rotor network in Fig. 1). The definition of state vectors $\boldsymbol{I}'$ and $\boldsymbol{\Phi}'(=\boldsymbol{L}_1'\boldsymbol{I}_1')$ are the same as $\boldsymbol{I}$ and $\boldsymbol{\Phi}$ except that the magnetic field H_ϕ' and vector potential A_z' of the rotor side on the interface are used.

D. Solution of the network equations

The transient analysis of the CLN is conducted by simultaneously solving the stator and rotor network equations (7) and (12). The state vectors of the stator and rotor are connected on the interface as $\boldsymbol{I}'=\boldsymbol{T}\boldsymbol{I}$ and $\boldsymbol{\Phi}'=\boldsymbol{T}\boldsymbol{\Phi}$, where $\boldsymbol{T}$ is the connection matrix derived from the boundary condition $H_\phi'=H_\phi$ and $A_z'=A_z$ [6]. The electromagnetic torque T_{e} is calculated as $T_{\mathrm{e}}=r_{\mathrm{c}}\boldsymbol{I}^{\mathrm{T}}\boldsymbol{B}$, where $\boldsymbol{B}$ is defined by the radial magnetic flux density $B_r=(1/r_{\mathrm{c}})\partial A_z/\partial\phi$ as $\boldsymbol{B}=\pi[A_{\mathrm{s}1},-A_{\mathrm{c}1},\cdots,(2K-1)A_{\mathrm{s}2K-1},-(2K-1)A_{\mathrm{c}2K-1}]^{\mathrm{T}}$.

E. Coupling with the equation of motion

The equation of motion of the rotor

$$J\frac{\mathrm{d}^2\theta_{\mathrm{m}}}{\mathrm{d}t^2}+D\frac{\mathrm{d}\theta_{\mathrm{m}}}{\mathrm{d}t}=T_{\mathrm{e}}-T_{\mathrm{L}} \tag{13}$$

is solved at each timestep with T_{e} obtained in II-D; T_{L} and θ_{m} are the load torque and mechanical angle, respectively; J and D are the moment of inertia and friction coefficient, respectively, of the rotor and load.

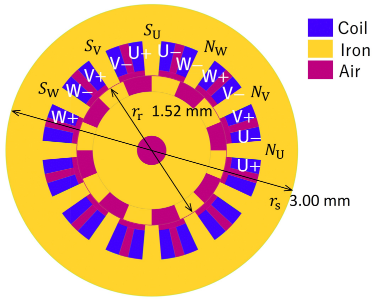

Fig. 2. Configuration of the VR stepper motor model analyzed in this study.

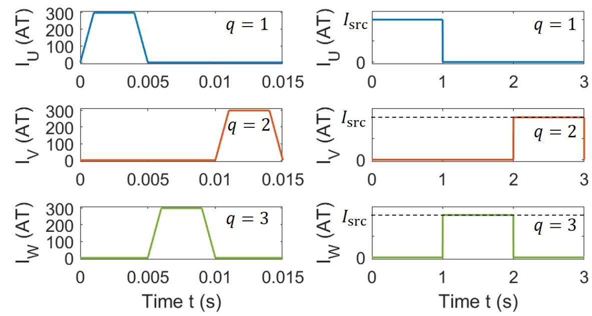

(a) (b)

Fig. 3. (a) Trapezoidal and (b) rectangular current inputs.

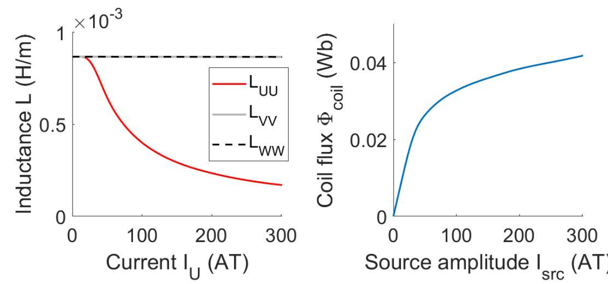

(a) (b)

Fig. 4. (a) Self-inductances L_{UU}, L_{VV}, and L_{WW} with $q = 1$. (b) Magnetic flux interlinking the coils.

III. Numerical Analyses

The concentrated-winding three-phase stepper motor, shown in Fig. 2, was analyzed. Although commercial VR stepper motors usually have more than a few dozen teeth, a simple model with eight rotor teeth and four stator poles was used in this study. The current direction (+ or -) when the amplitude is positive and the corresponding magnetic polarities (N and S) of the U, V, and W phases are also indicated in Fig. 2.

The stator iron-core was assumed to have the nonlinear reluctivity $\nu(\boldsymbol{B}) = \nu_i \left[h_1 \left(|\boldsymbol{B}|/B_0\right)^a + h_2\right]$, where $\nu_i = (1/4\pi) \times 10^3$ m/H, $a = 6$, $h_1 = 2$, $h_2 = 1$, and $B_0 = 1$ T. To study the effect of eddy current, we assumed that the rotor was bulk iron with a constant reluctivity and conductivity of $(1/4\pi) \times 10^4$ m/H and 1.0×10^6 S/m, respectively.

The inertia J and friction coefficient D were 1.0×10^{-4} kgm^2 and 5.0×10^{-5} Nms, respectively. The initial rotor angle and speed were $-\pi/36$ rad and 0 rad/s, respectively. A fan-type load torque $T_{\mathrm{L}} = b\Omega^3/|\Omega|$ Nm was assumed, where $\Omega = \mathrm{d}\theta_{\mathrm{m}}/\mathrm{d}t$ is the mechanical rotation speed.

The current inputs used in the simulation are shown in Fig. 3. From the configuration shown in Fig. 2, a continuous rotation in the counterclockwise direction is achieved by changing the index q in the sequence of $q = 1, 3, 2, 1, 3, 2, \cdots$.

A. Result of offline computation

Static offline calculations described in Section II-B and II-C were conducted before the transient analyses. We used the CLN consisting of three stages for the rotor. Thirty-two harmonic components composed the state vectors $\boldsymbol{I}$, $\boldsymbol{I'}$, $\boldsymbol{\Phi}$, and $\boldsymbol{\Phi'}$.

A lookup table of the stator inductance matrix $\tilde{\boldsymbol{L}}(\boldsymbol{\alpha})$ was created for three input indices ($q = 1, 2, 3$) and various amplitudes (I_{src} =0–301 AT, 10 divisions in the log scale for 4.77–301 AT). Fig. 4(a) shows the U, V, and W-phase self-inductances, L_{UU}, L_{VV}, and L_{WW}, which are the diagonal components of $L_{00}(\boldsymbol{\alpha})$ in (7). The results with $q = 1$ are shown. Only the U-phase current I_{U} was supplied, and L_{UU} decreased as I_{U} increased owing to the magnetic saturation. Conversely, L_{VV} and L_{WW} were almost constant; the effect of saturation was barely observed because of the salient structure of the stator teeth. Similarly, only L_{VV} and L_{WW} showed a noticeable decrease when q was 2 and 3, respectively. Fig. 4(b) shows the Φ_{coil} derived from (11) when $q = 1$. The same curve was obtained for $q = 2$ and 3 owing to the symmetric structure of the stator.

B. Result of online computation

The stator and rotor network equations coupled with the equation of motion were solved as described in Section II-D and II-E, where $\tilde{\boldsymbol{L}}(\Phi_{\mathrm{coil}}, q)$ was determined using cubic spline interpolation.

1) Continuous rotation

First, continuous rotation was simulated with the current input shown in Fig. 3(a) to demonstrate that the CLN method can handle variable amplitudes. The coefficient of the load torque b was 1.0×10^{-3}. Figs. 5(a) and (b) show the electromagnetic torque T_{e} and rotor angle θ_{m}, respectively, obtained using the parameterized CLN method (CLN), linear CLN method (CLN Lin.), and the FE analysis (FE). The results obtained using the parameterized CLN agreed well with the FE analysis, while those by the linear CLN were inaccurate.

2) Stepwise rotation and step-out motion

By adopting a longer switching time, we simulated stepwise rotation, a characteristic operation of stepper motors. The current input shown in Fig. 3(b) with a constant switching time 1 s and amplitude $I_{\mathrm{src}} = 20$ AT was assumed. $b = 5.0 \times 10^{-4}$ was used for the load torque. Fig. 6 includes the results obtained by the truncated network (Trunc.) Its rotor network consisted of only L_1', which represents the magnetostatic field, and the effect of the eddy current was not included. In Fig. 6(a), a large instantaneous torque was observed after the switching of the input. Fig. 6(b) shows the time evolution of the rotor angle, where the stepwise changes with oscillations were observed. The oscillation period of the CLN result agreed with the FE analysis better than the truncated network, which

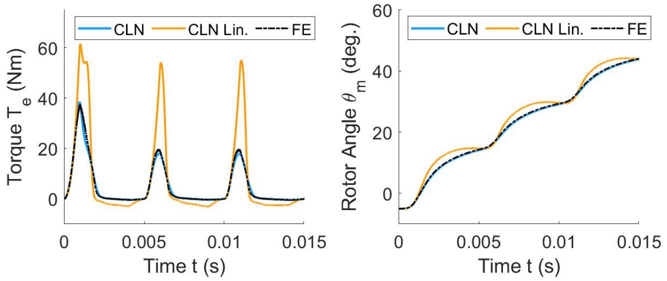

(a) (b)

Fig. 5. Time evolution of (a) electromagnetic torque and (b) rotor angle calculated using the parameterized CLN method (CLN), linear CLN (CLN Lin.), and FE analysis (FE).

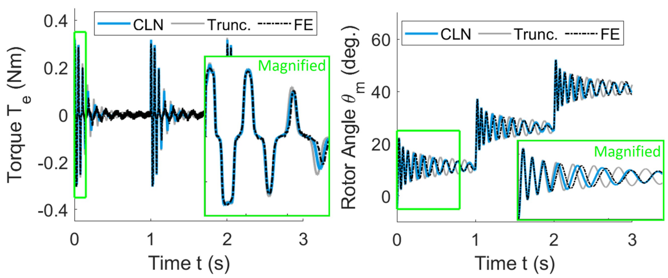

(a) (b)

Fig. 6. (a) Torque and (b) rotor angle of stepwise rotation. The results of the truncated network (Trunc.) are also shown.

indicates that the CLN method can accurately simulate the effect of eddy current in the rotor.

The step-out behavior was also analyzed. To observe the step-out motion, we employed smaller load torque with $b = 2 \times 10^{-5}$ and lower amplitude $I_{\mathrm{src}} = 5$ AT. The results until 2 s are shown in Fig. 7. The torque computed using the CLN and FE agreed well, as shown in Fig. 7(a). In Fig. 7(b), the stepwise motion was observed for the first sequence (0–1 s), where the rotor rotated by $15°$. However, when the current input was switched at 1 s, the oscillation was large enough to cause a step out, and the rotor angle transitioned in the negative direction. The CLN showed good agreement with the FE analysis, while the truncated network yielded an inaccurate result.

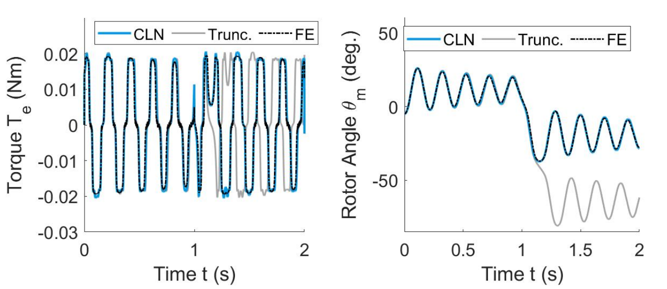

(a) (b)

Fig. 7. Time evolution of the (a) torque and (b) rotor angle when the load torque is small. A step-out motion is observed at $t = 1$ s.

C. Evaluation of computation time

The time consumed in the online calculation of the CLN method was negligible compared with the solutions of equations in the FE space. Therefore, we evaluated the computation time of the transient FE analysis and the offline calculations of the CLN by comparing the number of linear equations solved in the FE space.

The CLN method requires FE-space computations only for static offline calculations, and 1269 linear equations were solved, including iterations for solving nonlinear equations by the Newton–Raphson (NR) method. We also used the NR method in transient FE analyses, where the average number of iterations was 3.1 at each timestep. Therefore, the speed-up ratio of the CLN method to the FE analysis was $3.1N_{\mathrm{t}}/1269 \approx N_{\mathrm{t}}/409$, where N_t is the total number of timesteps. For the FE analyses shown in Figs. 5–7, N_{t} was 8000; hence, the speed-up ratio was 19.5. The ratio increases with a larger N_{t}, which means that the CLN method can be a powerful tool for studying various operating conditions during the coupling analysis with a control system.

IV. Conclusion

A nonlinear MOR of the VR stepper motor was constructed using the parameterized CLN method, whose transient analysis agreed well with those of the FE analysis. The parameterized CLN method was applicable to stepwise rotation and step-out motion analyses without any additional offline preparations. The CLN method was effective in reducing the computation time.

Acknowledgment

This study was partly supported by the Japan Society for the Promotion of Science under a Grant-in-Aid for Scientific Research (C) (No. 20K04443); and by JST, the establishment of university fellowships toward the creation of science, technology, and innovation (Grant No. JPMJFS2123).

References

[1] V. Mukherjee, M. F. Far, F. Martin, and A. Belahcen, “Constrained algorithm for the selection of uneven snapshots in model order reduction of a bearingless motor,” *IEEE Trans. Magn.,* vol. 53, no. 6, Art no. 7205304, 2017.

[2] S. Paul and J. Chang, “Fast numerical analysis of electric motor using nonlinear model order reduction,” *IEEE Trans. Magn.,* vol. 54, no. 3, Art no. 8101404, 2018.

[3] A. E. Boumesbah, F. Martin, G. Krebs, A. Belahcen, and C. Marchand, “Comparison of model order reduction methods for a switched reluctance machine characterization,” *IEEE Trans. Magn.,* vol. 57, no. 4, Art no. 7400906, 2021.

[4] A. Kameari, H. Ebrahimi, K. Sugahara, Y. Shindo, and T. Matsuo, “Cauer ladder network representation of eddy-current fields for model order reduction using finite-element method,” *IEEE Trans. Magn.,* vol. 54, no. 3, Art no. 7201804, 2017.

[5] T. Matsuo, K. Sugahara, A. Kameari, and Y. Shindo, “Model order reduction of an induction motor using a Cauer ladder network,” *IEEE Trans. Magn.,* vol. 56, no. 3, Art no. 7514704, 2020.

[6] M. Tobita and T. Matsuo, “Nonlinear model order reduction of induction motors using parameterized Cauer ladder network method,” *IEEE Trans. Magn.,* vol. 58, no. 9, Art no. 8205504, 2022.